DESY Summer Student Project

Investigation of the *in-situ* thermo-mechanical loading system at the beamline P02.1

Kuan-Ying Tseng

(DESY summer student 2018)

National Chiao Tung University, Taiwan

Email: ljoetseng@gmail.com

July 17 - Spetember 6, 2018

Supervisor:

Dr. Jo-Chi Tseng
Deutsches Elektronen Synchrotron DESY
FS-PE/PetraIII P02
Notkestr. 85
22607 Hamburg, Germany
Email: jochi.tseng@desy.de
Phone: +49-40-8998-5520

Abstract

Facing the problems of the destabilization of the heater and the inefficient heating circulation on the in-situ thermo-mechanical loading system at the beamline P02.1, two miniatures were designed and built. An in-situ heating experiment was carried out and temperature deviation between the set point and the sample was also calculated. Experimental temperatures of 25°C, 250°C, 300°C, 350°C, 400°C, and 450°C were conducted. The largest deviation temperature between the set point and the sample is 208°C. The refinement of the Proportional-Integral-Derivative (PID) parameter for the heating system was evaluated and tested comprehensively. Future work on minimizing the deviation temperature between the set point and the sample should be completed.

Contents

1 Introduction

In order to determine whether a newly developed material conforms to the requirements of mechanical stability and safety, it must undergo strict testing, especially tensile and compression testing. Furthermore, it is of great essence to disclose the change of micro-structure of the material during these testing [1]. With the advent of the synchrotron radiation, scientists are able to measure structural performances of the material at molecular scale. Compare to other experimental infrastructures, or the *in-house* X-ray in the laboratory, synchrotron radiation provides extremely strong beam light to transparent most of the samples non-destructively [2]. Accordingly, various *in-situ* experiments were carried out in the analysis of material structures of bio-molecules, composites and metals [3–5].

Hard X-ray Diffraction at beamline P02.1 at DESY offers a unfocused and collimated x-ray beam with size of ca. 0.6 (H) x 0.9 (V) mm^2 FWHM at an energy of 60 keV enabling users to conduct high resolution diffraction studies. Additionally, coupling mechanical loading with heating system at the beamline P02.1, users are capable of setting different environmental conditions to investigate material properties at distinct temperature. Under such circumstances, measurement of mechanical behavior, lattice expansion and deformation of a material can be conducted completely.

However, the experiment setup of *in-situ* thermo-mechanical loading system at beamline P02.1 met problems impeding users from acquiring effective data. First of all, the setup of the heater was unstable given that the heater was stabilized by simply two iron wires (see Figure 1. During the tensile/compression testing upon heating, the heater would shift resulting in blocking the beam. Secondly, the heating circulation system were required to be improved. To be more specific, through the figure showed in Figure 1, the heater provided heat source beneath the test bar causing uneven heating. The difference in temperature of both sides of test bar would create temperature gradient causing the inaccuracy of the measurement [6]. Therefore, The objective of this project is to resolve the problem for future need.

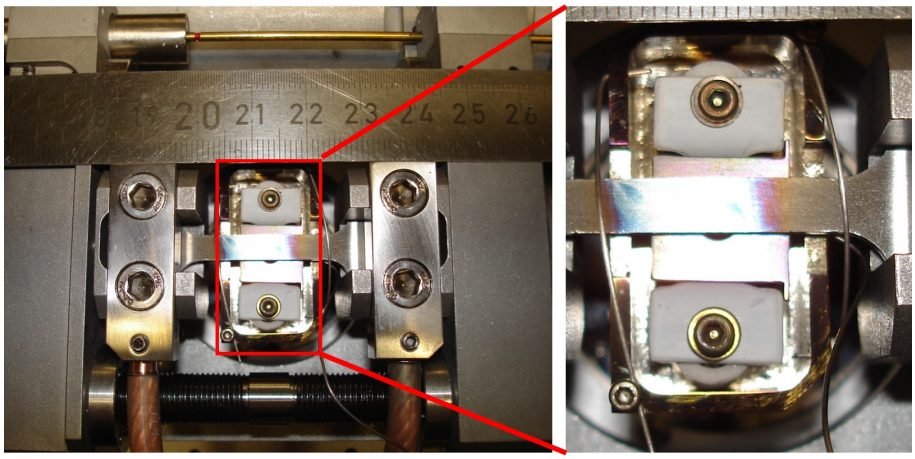

Figure 1: Heater setup on stress-rig

In this project, two miniatures were designed and built on the heating system. In-situ heating experiment was conducted for the purpose of discovering whether the upgraded heating system resolve the problem of temperature gradient. With the complete of this project, users are able to set up an experiment for strain mapping under thermo-mechanical loading at beamline P02.1.

2 *In-situ* thermo-mechanical loading system

2.1 *Introduction*

2.1.1 X-ray technique

The High Resolution Powder Diffraction beamline P02.1 operates at a fixed energy of 60 keV (corresponding to 0.207 Å) and exhibits low divergence, small energy bandwidth, and high flux [7]. The high-energy, monochromatic beam available at beamline P02.1 is perfectly suited for in-situ tensile/compression diffraction experiments. The use of high-energy photons is essential owing to the fact that it can minimize absorption effects in diffraction experiments in transmission mode as well as access to the characterization of nanocrystalline. Moreover, the high photon flux enables time resolved studies with resolution down to the (sub) second regime. As a result, structural and chemical transformations in this time regime can be effectively studied [7]. Figure 2 shows the layout of a typical experimental setup.

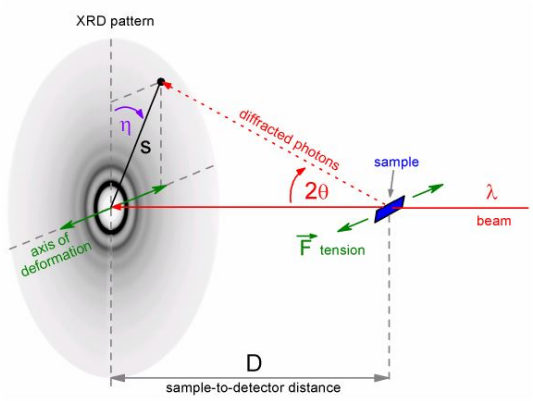

Figure 2: Typical layout of experimental setup

2.1.2 *In-situ* tensile experiment technique

The use of a 2-dimensional detector significantly improves the data statistics and thus makes it possible to get high-quality data. Figure 3 presents the setup of *in-situ* tensile experiments at beamline P02.1. The in-situ tensile experiment starts with the application of load to the desired value of macroscopic strain followed by performing x-ray scans at predefined positions with a small beam. The force is applied along the sample axis which is perpendicular to the incoming

beam. The load is increased in steps and the whole scanning procedure is repeated accordingly until the sample reaches its tensile fracture strength.

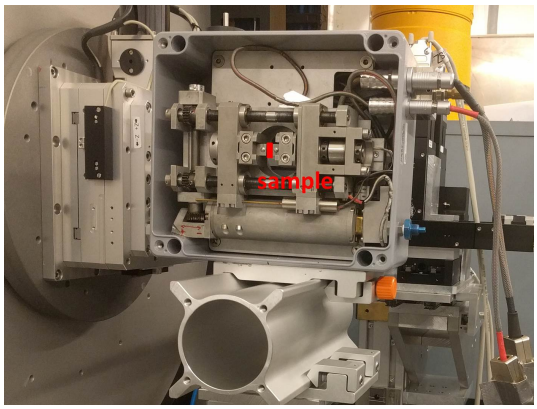

Figure 3: The tensile/compression unit from Kammrath & Weiss [8] installed at P02.1 beamline.

2.1.3 Scientific cases

Several *in-situ* X-ray diffraction experiments were implemetned for investigating the texture of polycrystalline materials upon deformation. X.D. Wang *et al.* [9] reported the difference in tensile behaviour of two bulk metallic glasses (BMGs), $Zr_{62}Al_8Ni_{13}Cu_{17}$ and $La_{62}Al_{14}(Cu_{5/6}Ag_{1/6})Co_5Ni_5$, by using *in-situ* X-ray diffraction. Figure 4(a) displays *in-situ* I(q) curves of the tensile direction for $Zr_{62}Al_8Ni_{13}Cu_{17}$ BMG with increasing tensile stress. The inset is the local magnification of the top part of the first peaks, showing that the peak positions change with stress in the tensile and transverse directions. Decrease of the peak position with increasing tensile stress (blue arrow in inset of Figure 4(a)) reflects the fact that atoms move apart along the tensile direction. An opposite behaviour is seen in transverse direction (red arrow in inset of Figure 4(a)).

Figure 4(b) shows the relationship between the tensile stress and the corresponding strain calculated by

$$\varepsilon = (q0 - q)/q \tag{1}$$

Where q0 and q refer to the positions of the first diffraction peak in I(q) under zero stress and stress σ, respectively. By linear fitting the points and calculating the ratio of strains between the transverse and tensile directions for each alloy, the tensile elastic modulus and Poisson' ratio can be obtained.

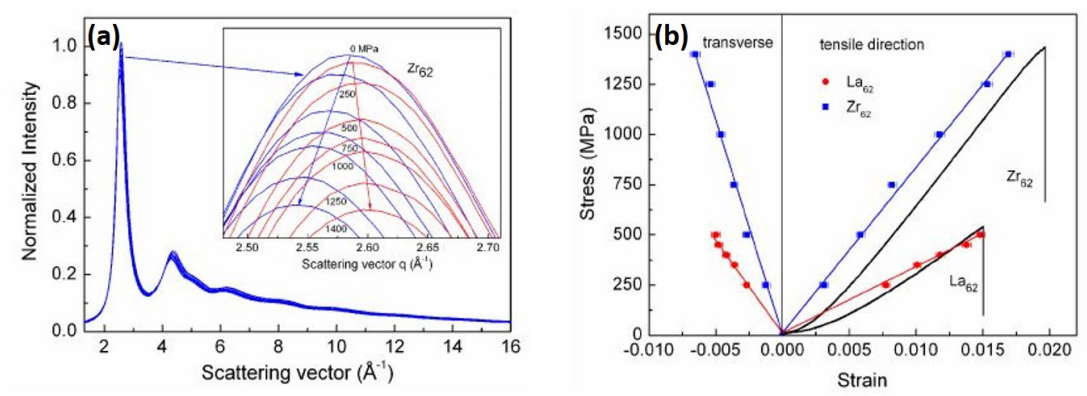

Figure 4: (a) Normalized diffraction curves I(q) of the tensile direction and the top part magnification of first peaks in I(q) of tensile/transverse directions changing with increasing stress for $Zr_{62}Al_8Ni_{13}Cu_{17}$. (b) Strains determined from the diffraction data of tensile/transverse directions. In addition, the room temperature tensile stress-strain curves of $Zr_{62}Al_8Ni_{13}Cu_{17}$ and $La_{62}Al_{14}(Cu_{5/6}Ag_{1/6})Co_5Ni_5$ BMGs are also included for comparison. Pictures taken from ref. 10.

Besides the investigation on tensile behaviour of BMGs through XRD technique, *in-situ* x-ray diffraction study were also proposed in different kinds of materials. Shijie Hao *et al.* [10] reported study in phase transformation of metal nanocomposite during tensile testing via high-energy XRD. Hao and his group discovered phase transformation of metal nanocomposite in distinct tensile cycle. Figure 5(a) reveals the retained B19' phase in the matrix. Upon removal of the pretreatment load, the plastically deformed Nb nanowires hindered the recovery of the NiTi matrix because of the B19'→B2 transformation, which caused large residual strains in the nanowires. Figure 5(b) denotes that upon unloading, the NiTi matrix underwent a reverse transformation from the stress-induced martensite to the parent phase.

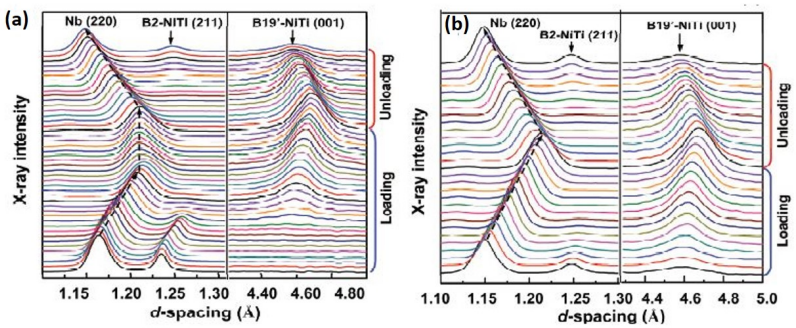

Figure 5: (a) Evolution of the diffraction peaks of Nb (220), B2-NiTi (211), and B19'-NiTi (001) during the pretreatment. (b) Evolution of the diffraction peaks of Nb (220), B2-NiTi (211), and B19'- NiTi (001) during the subsequent tensile cycle. The B2-versus-B19' peak intensity changes continuously, indicating continuous SIMT throughout the tensile loading. Pictures taken from ref. 11

In situ synchrotron XRD was not only widely used to characterize the deformation of the materials, but allows us to observe the phase transformation evolutions in the process of tensile experiment.

2.2 *Heating system*

2.2.1 Current status

Heating system on stress-rig at P02.1 beamline is combined with temperature controlling with the DDS microprocessor controller. Mainly, there are three parts of the system. First of all, the heater (see (1) in Figure 6), providing heat source from the bottom of the test bar, conducts heat from two ceramics to the Invar steel in the middle and finally the sample. Secondly, thermal couple (see (2) in Figure 6) is connected with the Invar steel to detect immediate temperature. Lastly, setup of the cooling water and two copper wires (see (3) in Figure 6) are essential owing to the stabilization of the temperature of whole system.

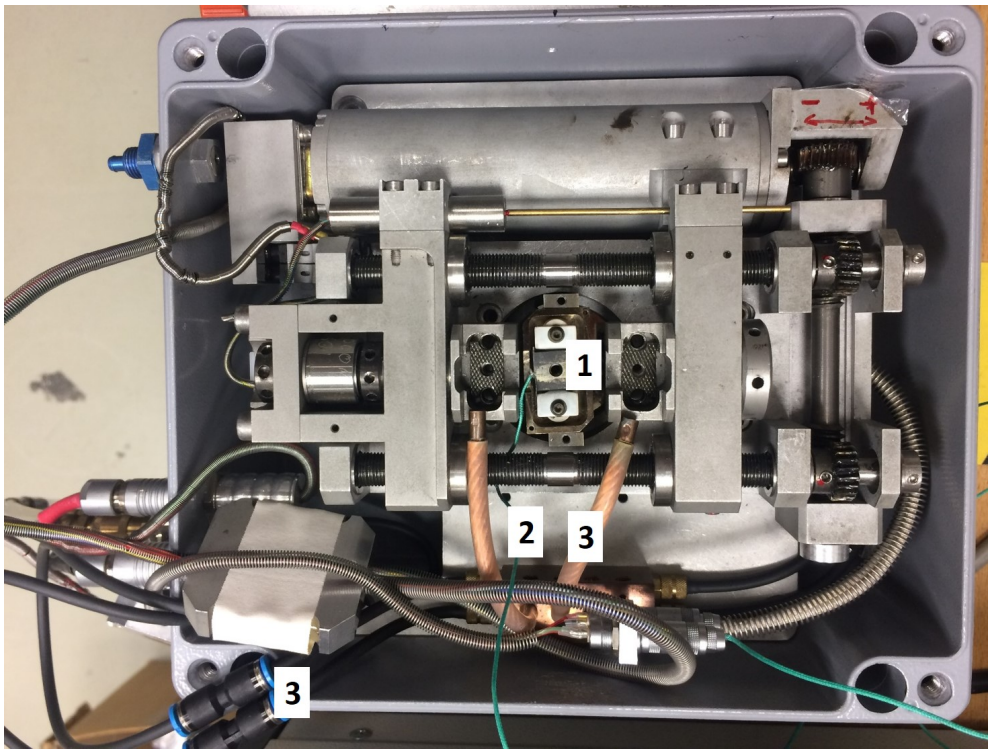

Figure 6: Heating system on the stress-rig - (1) heater, (2) thermal couple, (3) setup of the cooling water and two copper wires.

The controller allows different users' adjustments. Through refining the parameter setting in the PC program, users are able of finding the right temperature for their experiment. The method of refinement of PID parameters and the table of parameters for distinct temperatures will be explained and displayed in Section 3.3.

2.2.2 Upgrades

In order to resolve problems of stabilization of the heater and the uneven heating on the test bar, two miniatures on the heater were designed and built, which are the support frame and the cover. The design of the support frame is shown in Figure 7 and it relies on the structure of cooling stage at the bottom of the system (see Figure 8). During the experiment, the support frame can be perfectly fixed on the stage making the heater stable.

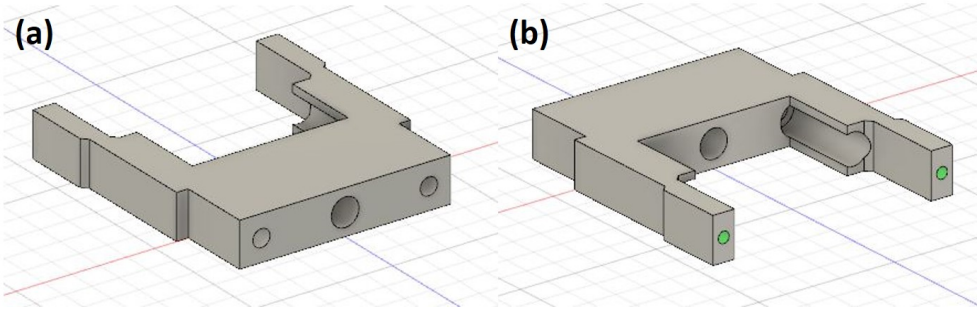

Figure 7: Support frame of the heater - (a) the bottom side connected to cooling stage, (b) the top side connected to heater.

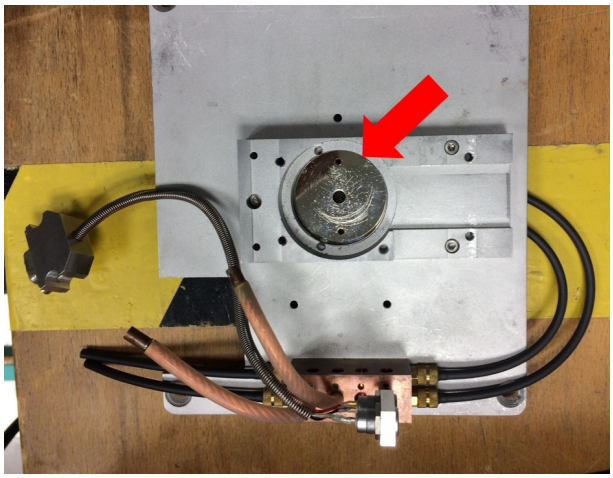

Figure 8: cooling stage

Furthermore, the cover on the heater (see Figure 9) was designed for the purpose of providing a favorable heating environment. With the cover, we are capable of establishing a window for heating circulation and minimize the effect of the temperature gradient. Figure 10 denotes the set-up of the updated heating system on stress-rig and the cross-section model of the designed structure. Finally, the experiment of confirming the improvement of the heating system was conducted and will be discussed in the following sections.

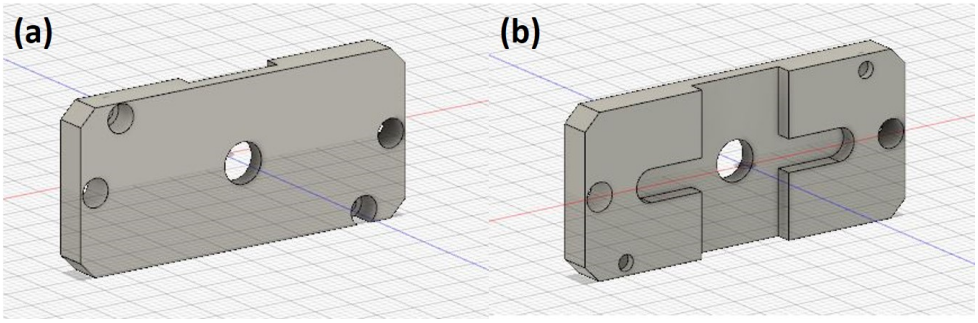

Figure 9: Cover of the heater - (a) the top side, (b) the bottom side.

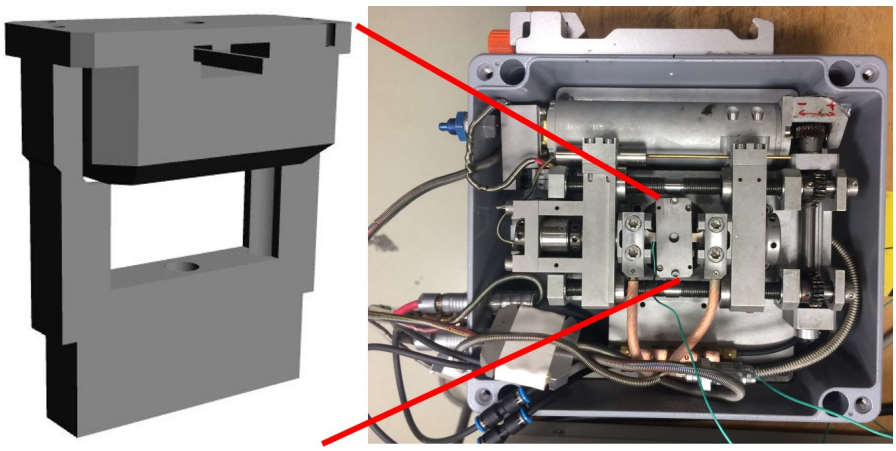

Figure 10: The cross-section model of the structure including the heater and the cover

3 Experiment and methods

3.1 *Sample preparation*

Certain dimension of sample is demanded for conforming to the tensile/compression testing on stress-rig. Size requirement of the sample is shown in Figure 11. For the in-situ heating experiment, a testing bar of titanium alloy produced by selective laser melting was prepared. In order to set up a standard data, we mixed Copper paste with Silicon on the top of the titanium alloy (see Figure 12).

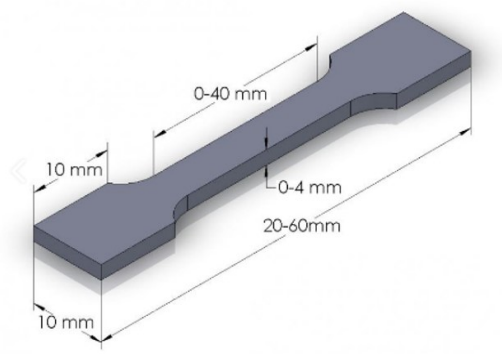

Figure 11: The size requirement of the sample

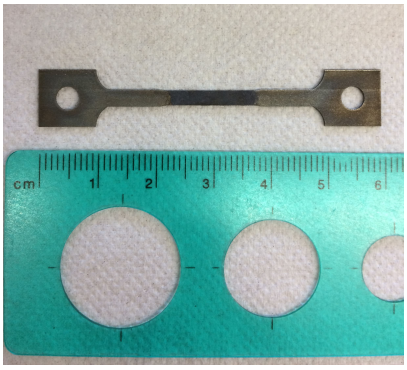

Figure 12: Titanium alloy with Copper paste mixed with Silicon

3.2 *Synchrotron X-ray diffraction*

Structural changes and phase transformations of metallic biomaterials during heating were examined by in situ synchrotron diffraction [11]. Different from the structure of hot-worked Ti6Al4V alloy containing two phases α (hcp) and β (bcc), Ti6Al4V alloy produced by selective laser melting possesses α' martensite in hcp phase [12]. At different temperatures of 25°C, 250°C, 300°C, 350°C, 400°C, and 450°C, the same position of the sample were irradiated by x-ray radiation with the wavelength of 0.20733 Å (59.8 keV) at beamline P02.1, DESY. Diffraction patterns were integrated into one dimension from the 2D detector. The lattice expansion of two phases acquired by XRD is capable of evaluating the thermal expansion coefficient of Ti6Al4V alloy and the performance of thermal conductivity.

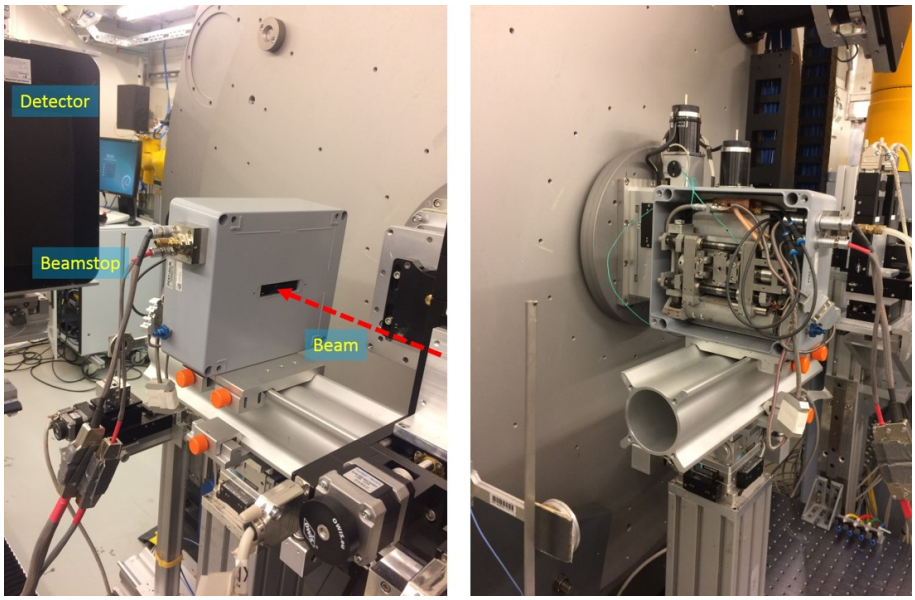

Figure 13: Experiment setup

3.3 *Refinement of PID parameters*

Briefly introduction of the definition of different parameters is provided. However, for further details, users have to look up in Module 5000N user's handbook [13].

Proportional-Integral-Derivative (PID) control is the most common algorithm used in industry and has been universally accepted in industrial control. As the name suggests, PID algorithm consists of three basic coefficients; proportional, integral and derivative which are varied to get optimal response [14]. Except these three coefficients, the settings for experiment temperature and the maximum heating voltage are also required in this heating system. Information down below are the definition of different parameters.
BL = maximum heating voltage (0 - 15 V)
P = % of BL per °C deviation from required temperature
I = integral, the time between comparison and control action
D = Reaction to disturbance
To prevent "overshooting", that is unwanted oscillations with the parameter the user first trued, then set P, I, and D to zero and increase BL. With further increase, users will get nearly the temperature they need, except the process is low. To keep the temperature stable along with set point, the correction of the P, I, and D is of great importance.

Parameters for different temperatures are evaluated from the tests and shown in Table1.

Table 1: Refinement of PID parameters according to different temperatures

Set point [°C]	BL	P	I	D
200	6.0	5.0	20.0	2.0
250	7.0	4.0	30.0	1.0
300	8.0	3.0	30.0	2.0
350	9.0	3.0	30.0	3.0
400	9.0	5.0	20.0	2.0
450	9.0	7.0	30.0	2.0

4 Results & Discussion

In order to comprehend whether the upgraded heating system meet the demand for the in-situ thermo-mechanical loading experiment, we calculated temperature deviation between the set point temperature and the temperature of the sample. The data of the set point temperature was acquired from a thermocouple, while the temperature of the sample was analyzed by the one dimensional diffraction pattern. Through Bragg's law:

$$n\lambda = 2d\sin\theta \tag{2}$$

We are capable of calculating the lattice constant from the given theta. In addition, through the formula of thermal expansion:

$$\frac{\Delta d}{d} = \alpha_L \Delta T \tag{3}$$

The thermal expansion coefficient of titanium alloy, which is $1.17 \times 10^{-5}\, K^{-1}$ [15], the temperature of the sample can be calculated. The diffraction pattern of the titanium alloy was collected at 10 seconds/point with 10 consecutive points when the set point temperature was stable. Table2 displays the temperatures of the set points and the relative temperatures of titanium alloy. From the table, the deviation temperature between the set point temperature and the temperature of titanium alloy upon heating is from 144°C to 208°C. The data in table 2 is plotted below in Figure 14. The large deviation of the temperature can be attributed to the short heating time. Further experiment should be carried out for clarification.

Table 2: Comparison of temperatures detected from thermocouple, and temperatures analyzed from Ti64 diffraction pattern

Set point [°C]	$T_{thermocouple}$	T_{Ti64}	Temp. deviation
250	250(0.2)	104(1.2)	144
300	300(0.5)	132(0.8)	168
350	350(0.2)	167(1.1)	183
400	400(0.3)	192(3.8)	208
450	450(0.2)	243(2.0)	207

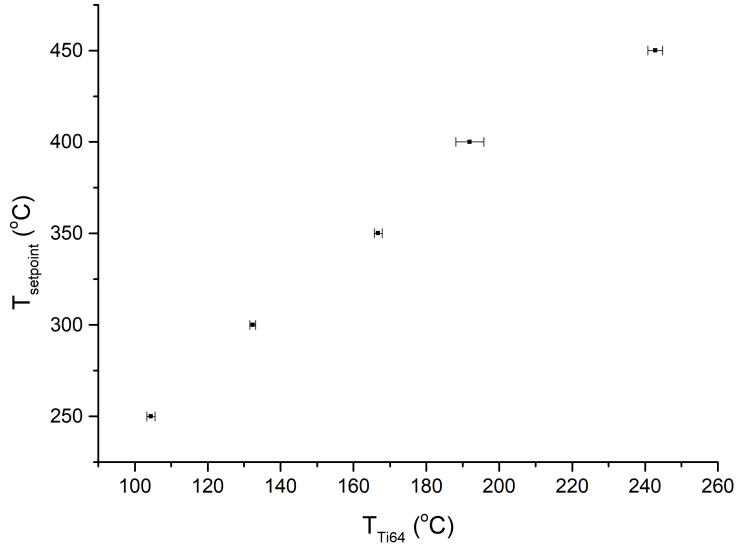

Figure 14: The relative temperature between the set point and the sample

5 Conclusion

Two miniatures were designed and built on the heating system for resolving the problems of the destabilization of the heater and the unfavorable heating circulation system on in-situ thermo-mechanical loading system at beamline P02.1. Problem of stabilization of the heater was ameliorated. However, from the in-situ heating experiment, the maximum deviation temperature between the set point temperature and the temperature of titanium alloy upon heating went up to 208°C, which can be attributed to the short heating time. Significant modification of the system is needed for future work. The completion of the refinement of PID parameters enables users to conduct experiments at ideal temperature. Further experiments are required for ensuring the implement of the in-situ thermo-mechanical loading experiment for users at beamline P02.1.

6 Acknowledgement

Mainly, I would like to express big thanks to my supervisor Dr. Jo-Chi Tseng for supporting me and giving me crucial advises on my project. I would also like to thank Sergeh Wenz and Martin Etter for discussing the design for the heating system with me. Specially thanks to Sergeh Wenz for completing the product efficiently and proficiently. I do appreciate the support from Tim Schoof, especially his experience on programming. I am grateful for all the support from P02.1 group, including Michael Wharmby, Jozef Bednarcik, and Alexander Schökel. Finally, my sincere thanks goes to all organizers of the DESY Summer Student Programme 2018, to all our lectures and to all participants for such a wonderful experience.

7 Appendix

User's Manual

For users who are interested in conducting High-Energy X-ray Strain Mapping under Thermal-mechanical Loading, here we provide a manual for you.

Step1. Setting up heating system on the stage

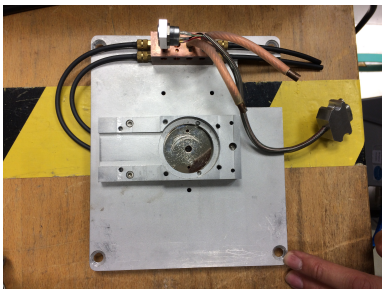

Step2. Lock the support of the heater on the cooling stage and set up the heater

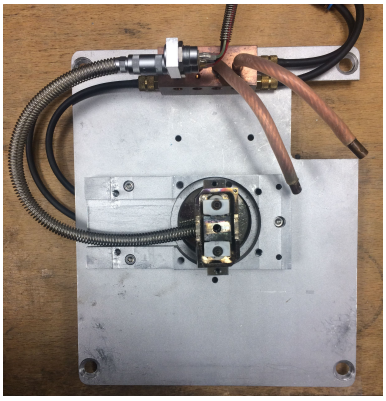

Step3. Connect the thermal couple with the heater before setting the position of the sample

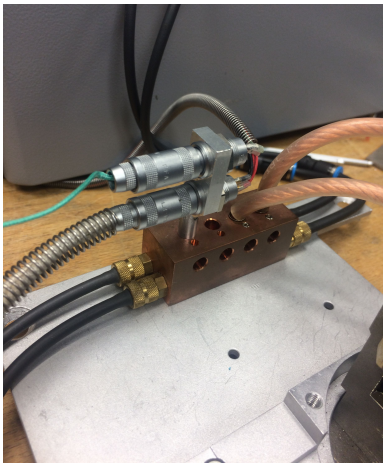

Step4. Place the system in the box and connect copper wire and cooling water

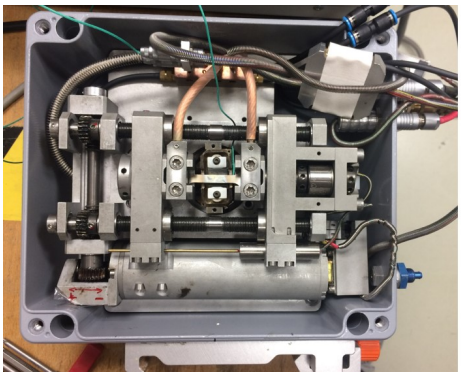

Step5. Set the cover on the heater and connect the cable to DDS controller

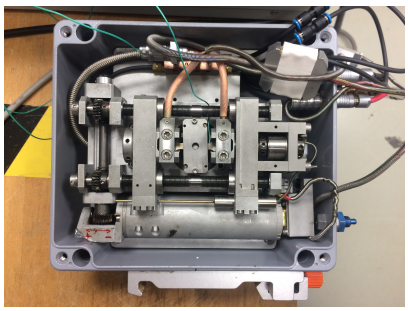

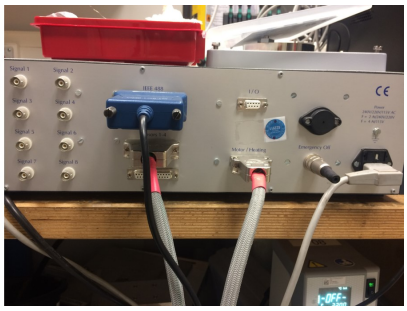

Step6. Operate the DDS Microprocessor Controller from the computer

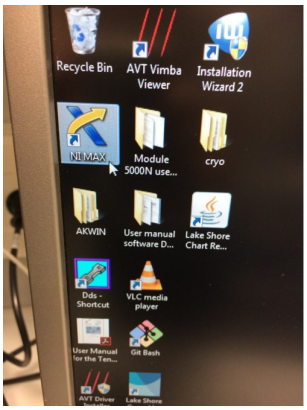

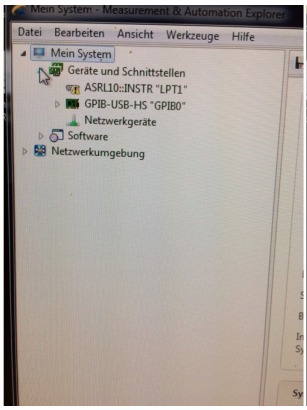

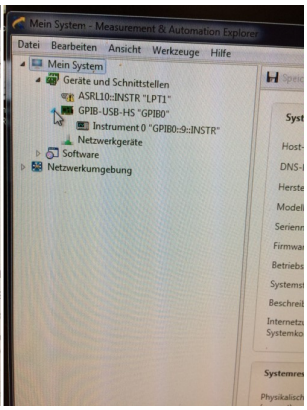

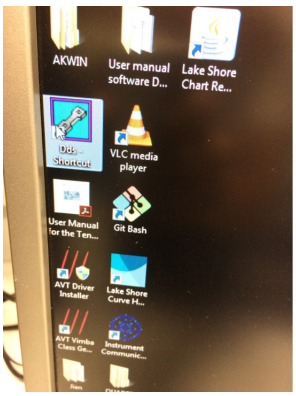

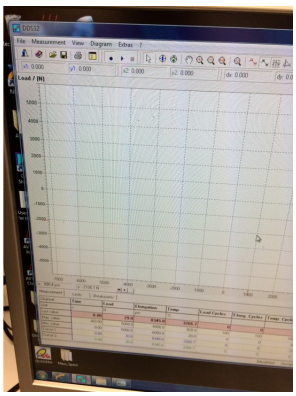

P.S.

- The length of middle part of dog-bone shaped specimen has to be more than 20 mm
- The maximum tensile load is 5000N
- Do not set the elongation rate over 20 micrometer/second
- For more details regarding how to set up the elongation rate, the maximum tensile load, and the maximum elongation length, etc., please look up in the Module 5000N user's handbook.

References

[1] R. F. Landel and L. E. Nielsen, *Mechanical Properties of Polymers and Composites, Second Edition*, Google-Books-ID: l0xUDwAAQBAJ (CRC Press, Dec. 14, 1993), 573 pp.

[2] V. A. Bordovitsyn, *Synchrotron Radiation Theory and Its Development: In Memory of I M Ternov*, Google-Books-ID: CKNIDQAAQBAJ (World Scientific Publishing Company, July 5, 1999), 479 pp.

[3] M. Weik, R. B. G. Ravelli, G. Kryger, S. McSweeney, M. L. Raves, M. Harel, P. Gros, I. Silman, J. Kroon, and J. L. Sussman, "Specific chemical and structural damage to proteins produced by synchrotron radiation", PNAS **97**, 623 (2000).

[4] G. A. WlvcnuNls, "Synchrotronradiation xANESspectroscopyof Ti in minerals: Effects of Ti bondingdistances,Ti valence,and site geometryon absorptionedgestructure", 13.

[5] A. Kirfel and K. Eichhorn, "Accurate structure analysis with synchrotron radiation. The electron density in Al2O3 and Cu2O", Acta Crystallographica Section A **46**, 271 (1990).

[6] T. Hashimoto, J. Bodycomb, Y. Funaki, and K. Kimishima, "The Effect of Temperature Gradient on the Microdomain Orientation of Diblock Copolymers Undergoing an Order–Disorder Transition", Macromolecules **32**, 952 (1999).

[7] *High Resolution Powder Diffraction Beamline P02.1*, `http://photon-science.desy.de/facilities/petra_iii/beamlines/p02_hard_x_ray_diffraction_beamline/hrpd/index_eng.html`.

[8] *Tensile/Compression Module*, `https://www.kammrath-weiss.com/en/products/materials/tensile-compression.html`.

[9] X. D. Wang, J. Bednarcik, K. Saksl, H. Franz, Q. P. Cao, and J. Z. Jiang, "Tensile behavior of bulk metallic glasses by *in situ* x-ray diffraction", Applied Physics Letters **91**, 081913 (2007).

[10] S. Hao et al., "A Transforming Metal Nanocomposite with Large Elastic Strain, Low Modulus, and High Strength", Science **339**, 1191 (2013).

[11] M. Bönisch, A. Panigrahi, M. Stoica, M. Calin, E. Ahrens, M. Zehetbauer, W. Skrotzki, and J. Eckert, "Giant thermal expansion and α-precipitation pathways in Ti-alloys", Nature Communications **8**, 1429 (2017).

[12] K. Wissenbach, S. Höges, P. Robotti, A. Molinari, L. Facchini, and E. Magalini, "Ductility of a Ti-6Al-4V alloy produced by selective laser melting of prealloyed powders", Rapid Prototyping Journal **16**, 450 (2010).

[13] *Module 5000N user's handbook*, July 2006.

[14] *PID Theory Explained - National Instruments*, `http://www.ni.com/white-paper/3782/en/#toc2`.

[15] A. K. Swarnakar, O. Van der Biest, and B. Baufeld, "Thermal expansion and lattice parameters of shaped metal deposited Ti–6Al–4V", Journal of Alloys and Compounds **509**, 2723 (2011).